Available online at www.sciencedirect.com
SCIENCE DIRECT®
Bioorganic & Medicinal Chemistry 13 (2005) 4007–4013
Bioorganic & Medicinal Chemistry

Synthesis and biological evaluation of aromatic enones related to curcumin

Thomas Philip Robinson,[b] Richard B. Hubbard, IV,[b] Tedman J. Ehlers,[b] Jack L. Arbiser,[c] David J. Goldsmith[d] and J. Phillip Bowen[a,*]

[a]*Center for Drug Design, Department of Chemistry and Biochemistry, University of North Carolina at Greensboro, 400 New Science Building PO Box 26170, Greensboro, NC 27402, USA*
[b]*Center for Biomolecular Structure and Dynamics, Department of Chemistry, University of Georgia, Athens, GA 30602, USA*
[c]*Department of Dermatology, Emory University School of Medicine, 5007 Woodruff Memorial Building, Atlanta, GA 30322, USA*
[d]*Department of Chemistry, Emory University, Atlanta, GA 30322, USA*

Received 9 March 2005; revised 30 March 2005; accepted 30 March 2005
Available online 28 April 2005

Abstract—Curcumin, a natural product isolated from the spice turmeric, has been shown to exhibit a wide range of pharmacological activities including certain anti-cancer properties. It has been specifically shown to be an effective inhibitor of angiogenesis both in vitro and in vivo. Using curcumin as a lead compound for anti-angiogenic analog design, a series of structurally related compounds utilizing a substituted chalcone backbone have been synthesized and tested via an established SVR cell proliferation assay. The results have yielded a wide range of compounds that equal or exceed curcumin's ability to inhibit endothelial cell growth in vitro. Due to both their commercial availability and their fairly straightforward synthetic preparation, these low molecular weight compounds are attractive leads for developing future angiogenic inhibitors.

1. Introduction

Cancer is a general term used to describe many disease states, each of which is characterized by abnormal cell proliferation. The causes, which bring about this abnormal cellular behavior are specific to each type of cancer. The success of tumor-targeted therapy is limited by this inherent dissimilarity. One common denominator for all types of cancer is the requirement of a stable blood supply. Therefore, tumor vasculature has been identified as a potential target for therapeutic intervention.

Angiogenesis is the process by which new capillaries are formed from the body's existing vascular system. It is typically a quiescent process that is only made active in conjunction with menstruation and wound healing in adults. When it does take place outside of these limited boundaries, it is typically due to a disease process. Angiogenesis is present, and in fact instrumental, in a wide range of disease states including arthritis, corneal ulceration, psoriasis, and tumor growth. Although it is not essential during the initial stages of tumor formation, neovascularization is vital for the continued survival and growth of a developing tumor mass. Without an adequate blood supply to provide it with oxygen and an efficient means of disposing of waste products, the tumor will be unable to grow larger than 1–2 mm in diameter. Along with a stable supply of blood, fresh capillary invasion of the tumor mass also introduces the possibility of metastasis.

The process of angiogenesis is multifaceted. Prospective therapeutic strategies can focus on several key aspects of the process: blocking the degradation of the basement membrane (metalloproteinase inhibitors), maintaining the equilibrium between biochemical angiogenic promoters and inhibitors, and the direct inhibition of endothelial cell proliferation (TNP-470, thalidomide, squal- amine, and endostatin).

Curcumin, also known as diferuloylmethane, is a carotenoid pigment isolated from the spice turmeric. Its structure is provided in Figure 1. Turmeric itself is originally obtained from the powdered rhizome of the plant *Curcuma longa* L.[1,2] Curcumin, the major bioactive

Keywords: Curcumin; Angiogenesis; Chalcone; Enone.
* Corresponding author. Tel.: +1 336 334 4257; fax: +1 336 334 5402; e-mail: jpbowen@uncg.edu

0968-0896/$ - see front matter © 2005 Elsevier Ltd. All rights reserved.
doi:10.1016/j.bmc.2005.03.054

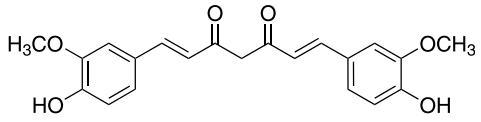

Figure 1. Structure of curcumin.

component of turmeric, has been shown to exhibit a wide range of interesting biological activities including anti-oxidant,[3,4] anti-inflammatory,[5,6] and anti-HIV properties.[7,8] Perhaps most importantly, it has also exhibited significant anti-tumor activity. Curcumin has been shown to inhibit the progression of artificially induced skin and colon cancers in animal models.[9–13] Both of these forms of cancer differ significantly in their genetic basis, which lead researchers to postulate that curcumin's ability to hinder the progression of these distinct cancer types is based on its ability to inhibit angiogenesis. Arbiser et al. discovered soon after that curcumin inhibits basic fibroblast growth factor (bFGF)-induced endothelial cell proliferation in vitro and does, in fact, inhibit angiogenesis in vivo.[14]

Although the specific mechanism by which curcumin enacts its regulation of the angiogenic process is not currently known, its efficacy in doing so, coupled with its relatively straightforward chemical structure, has made it an attractive lead compound for structure modification and drug development studies. The efforts to date have centered mostly on the truncation of the central region of the molecule from a β-diketone to a more compact enone linker. This, coupled with modifications to the size and substitution patterns of the two aromatic ring moieties present in the molecule, has yielded a number of highly effective curcumin analogs, which show impressive anti-proliferative activity against SVR endothelial cells in vitro.[15–17]

2. Results and discussion

It has been postulated that the biological efficacy of curcumin arises from the electrophilic nature of its central β-diketone component.[15,16] The enone derivatives selected for investigation retain this essential characteristic, while at the same time simplifying the overall structure of the molecule. In an effort to develop a robust pharmacophoric model and understand the basis for biological activity, the molecular structure of curcumin can be subdivided into three key regions: two substituted aromatic moieties (A and C) joined together by a conjugated β-diketone linker (B) [see Fig. 2].

By dividing the molecule into specific and modifiable regions of interest, a simple, yet effective, pharmacophore model for the curcumin analogs was developed. Each individual region can be modified independently of the others in order to aid in the systematic refinement of the search for increasingly effective curcumin derivatives. In the current study, compounds with an abbreviated linker between the two aromatic regions comprised the primary focus. The linker was shortened from curcumin's original β-diketone to a more compact singular enone moiety (B′) [see Fig. 3]. Figure 4 is a generalized representation of the pharmacophore substitution patterns. Working within this new molecular framework (A′, B′, C′), a variety of mixed aromatic systems and substitution patterns were either obtained from commercial sources or synthesized in the laboratory. The biological efficacy as an in vitro inhibitor of endothelial cell proliferation was evaluated for each compound via the previously described Arbiser SVR cell assay.

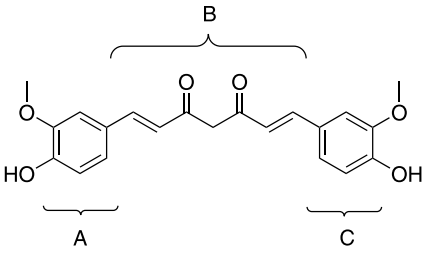

Figure 2. Key structural regions of curcumin.

Curcumin has previously been shown to inhibit in vitro SVR endothelial cell growth by 41.5% at 1 μg/ml, 37.8% at 3 μg/ml, and 56.2% at 6 μg/ml. These values were used as a benchmark by which to judge the relative effectiveness of the synthesized derivatives. The prototypical aromatic enone, chalcone (**1**), was the first enone analog tested, as it possessed all of the fundamental characteristics required for the proposed pharmacophore.

Chalcone inhibits SVR cell growth by 71.6% at 1 μg/ml, 92.8% at 3 μg/ml, and 94.4% at 6 μg/ml. This was a very encouraging piece of datum as it proved that even with

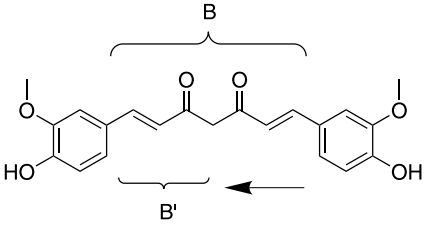

Figure 3. Proposed modification of curcumin's β-diketone linker region.

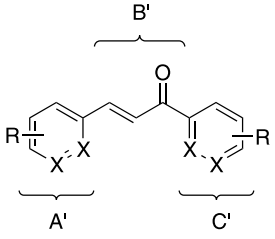

Figure 4. Generalized substitution patterns of the aromatic enone analogs investigated. R = Cl, F, CH_3, NO_2, isopropyl, OBn, phenyl, OCH_3, and OH; X = C, N; A′ and C′ = benzene, pyridine, furan, pyrrole, naphthalene, anthracene, biphenyl, and benzo[1,3]dioxole.

the simplified framework, the aromatic enone analogs still retain the fundamental characteristics required for biological potency. In fact, a large number of the enone analogs investigated either matched or exceeded curcumin's levels of in vitro cell inhibition. Overall, 63 different analogs were obtained and tested. Their structures and the corresponding inhibition data are presented in Tables 1–5. Each table represents a specific subset of the enone analogs. Tables 1–4 contain derivatives differing in either the substitution pattern of the benzene rings or the type of aromatic moiety utilized (benzene, pyrrole, pyridine, furan, naphthyl, anthryl, biphenyl, and benzo[1,3]dioxole). Table 5 presents the data obtained from the tetralone analogs included in the study. The tetralone derivatives introduced a measure of rigidity to the central enone moiety of the compounds. The 2-naphthyl analog (**61**) showed very promising results.

Table 1. Percent inhibition of in vitro endothelial cell proliferation for enone analogs

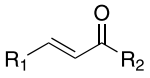

Compd	R1	R2	SVR growth inhibition		
			1 μg/ml	3 μg/ml	6 μg/ml
1			71.6	92.8	94.4
2			29.9	40.2	58.5
3			73.7	98.2	98.1
4	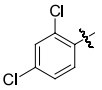		19.9	10.4	84.7
5	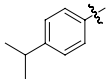		19.5	14.2	59.2
6			47.7	57.9	89.6
7			36.3	67.3	89.5
8			41.7	80.4	87.3
9			29.6	25.3	73.4
10	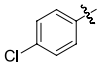		13.8	11.7	31.1
11		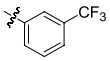	42.3	87.4	96.9
12	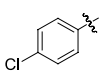		22.3	24.5	46.5

Table 1 (*continued*)

Compd	R1	R2	SVR growth inhibition		
			1 μg/ml	3 μg/ml	6 μg/ml
13			48.3	75.3	93.7
14	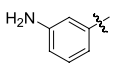	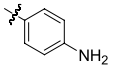	43.5	38.1	69.1
15	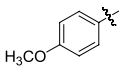	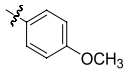	29.1	63.4	85.2
16			4.6	61.0	94.0
17			2.2	51.1	88.7
18		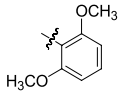	23.2	43.7	52.3
19	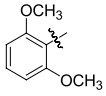		31.8	56.4	60.8
20			25.8	39.8	63.5
21			36.2	49.2	39.2
22			40.7	89.1	96.9
23			30.3	31.7	83.2
24			0.0	53.4	85.2
25			12.6	0.0	5.3
26			13.7	3.8	29.7
27			31.1	88.6	88.6
28			47.6	70.3	84.5
29			0.0	0.0	0.0
30			6.6	55.6	88.7

Table 2. Percent inhibition of in vitro endothelial cell proliferation for naphthyl/anthryl/*p*-phenyl analogs

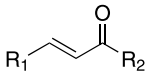

Compd	R1	R2	SVR growth inhibition		
			1 μg/ml	3 μg/ml	6 μg/ml
31		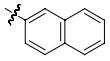	0.0	78.7	88.6
32	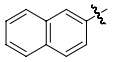		0.0	75.4	66.2
33		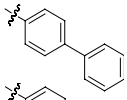	10.4	34.7	0.0
34	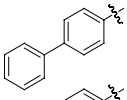	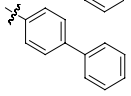	19.2	0.0	0.0
35	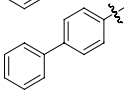		24.9	12.9	41.4
36		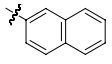	12.2	35.3	96.8
37	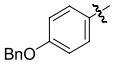	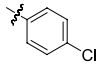	25.6	4.4	62.9
38	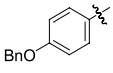		18.4	5.1	17.0
39		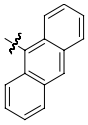	25.5	46.4	69.0
40	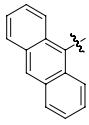		54.6	53.5	71.3
41	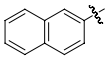	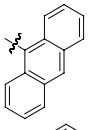	52.5	57.3	48.1
42			10.9	33.2	68.2
43	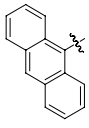	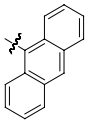	0.0	0.0	4.7
44		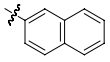	0.0	24.9	50.3
45	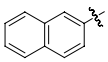	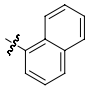	0.0	22.4	52.0
46			12.0	55.5	60.3

Even at the lowest concentration, it exhibited over 80% inhibition.

Table 3. Percent inhibition of in vitro endothelial cell proliferation for 5-benzo[1,3]dioxole analogs

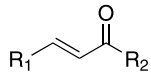

Compd	R1	R2	SVR growth inhibition		
			1 μg/ml	3 μg/ml	6 μg/ml
47	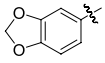	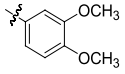	1.9	24.2	48.1
48	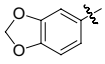	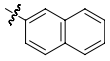	5.7	1.4	11.9
49	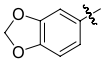		21.3	0.0	0.0
50			1.0	14.4	45.5
51			36.5	12.7	24.5
52			31.0	34.3	80.8
53			33.0	32.5	68.9
54			28.3	44.1	78.4

Table 4. Percent inhibition of in vitro endothelial cell proliferation for aromatic five membered ring analogs

Compd	R1	R2	SVR growth inhibition		
			1 μg/ml	3 μg/ml	6 μg/ml
55			7.7	8.1	12.0
56			9.8	1.0	0.0
57			28.2	57.7	90.2
58			8.3	11.4	19.4
59			19.0	21.5	0.4

A number of the most active chalcone analogs, 2,6-dichloro-4′-methylchalcone (**3**) for one, bear electron withdrawing groups on the *ortho* position(s) of their aromatic rings. Several of the other top rated analogs possess either an *ortho* positioned heterocycle or, in the case of the tetralone derivatives, an extra cyclohexanone ring that could result in significant steric strain for the molecule if it were to adopt a planar orientation. This suggests that such substitution may force the aromatic rings out of conjugation with the enone moiety, thereby isolating it and increasing its overall electrophilic char-

Table 5. Percent inhibition of in vitro endothelial cell proliferation for tetralone analogs

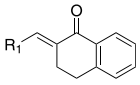

Compd	R1	SVR growth inhibition		
		1 μg/ml	3 μg/ml	6 μg/ml
60		5.7	11.4	40.8
61	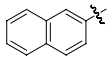	84.7	84.9	78.8
62		32.8	37.0	53.7
63		1.0	76.4	52.1

acter, subsequently making it more susceptible to nucleophilic attack. As a further test of the necessity of the electrophilic enone moiety in the test compounds, 1,3-diphenyl-1-propanone was synthesized and evaluated. Its comparatively low level of activity (5.1% at 1 μg/ml, 0% at 3 μg/ml, and 11.5% at 6 μg/ml) lends credence to the purported importance of the enone moiety's presence in the curcumin analogs.

2.1. Conclusions and future research

With the recent discovery that curcumin may achieve its antiangiogenic activity via the inhibition of an aminopeptidase,[18] the potential for future fine tuning of the pharmacophore utilizing molecular modeling packages is very promising. With a possible active site identified, modeling efforts could greatly aid in the search for the ideal angiogenic inhibitor. Potential drug choices could be assessed via docking studies prior to their synthesis in order to pre-evaluate their binding potential. Computational studies are currently underway in an effort to build a structure–activity relationship profile utilizing the current crop of inhibitors described herein.

3. Experimental

The chalcone derivatives presented in Tables 1–5 were each prepared according to a similar synthetic procedure. The synthesis of the target compounds employed traditional Claisen–Schmidt reaction conditions. The reported α,β-unsaturated ketone products are a result of a base induced condensation of the appropriate aromatic aldehydes and ketones.

General synthetic procedure: Equimolar portions of the appropriately substituted aromatic aldehydes (10 mmol, 1 equiv) and ketones (10 mmol, 1 equiv) were dissolved in approximately 15 ml of ethanol. The mixture was allowed to stir for several minutes at 5–10 °C (ice bath). A 10 ml aliquot of a 40% aqueous potassium hydroxide solution was then slowly added dropwise to the reaction flask via a self-equalizing addition funnel. The reaction solution was allowed to stir at room temperature for approximately 4 h. Most commonly, a precipitate formed and was then collected by suction filtration. Recrystallization from the appropriate solvent afforded the pure product. In certain instances, a solid product was not obtained by the end of the reaction period (monitored by TLC). Two alternate strategies were employed in order to isolate the target compounds. First, the reaction was neutralized with a dilute acid solution in an effort to aid the product's precipitation from solution. If this method was not successful in producing a precipitate, the solution was then extracted with either anhydrous ether or chloroform (three portions, ~10 ml). The organic layers were collected and concentrated using a rotoevaporator to afford the crude product. Recrystallization and/or column chromatography was then utilized to purify the desired product (Scheme 1).

Several variations of this general procedure were utilized in order to obtain the test compounds. Each variation has been illustrated with a specific example.

3.1. 2′,6′-Dimethoxychalcone (20)

To a solution of benzaldehyde (295 mg, 2.77 mmol) and 2,6-dimethoxyacetophenone (500 mg, 2.77 mmol) in 4.1 ml of methanol was added 0.1 ml of 40% sodium hydroxide in water at 10 °C. After stirring for 1 h at room temperature, a solid appeared and was filtered. The precipitate was recrystallized from methanol to afford 371 mg (49.9%) of white flakes: mp 125.5–126.6 °C (lit. mp 123–124 °C). ^{1}H NMR (250 MHz) δ 7.55–7.51 (m, 2H), 7.39–7.30 (m, 5H), 7.00–6.94 (d, 1H), 6.64–6.61 (d, 2H), 3.79 (s, 6H); ^{13}C NMR (62.7 MHz) 213.8, 176.1, 163.9, 153.4, 149.4, 149.0, 147.4, 147.3, 147.0, 122.6, 74.5 ppm.

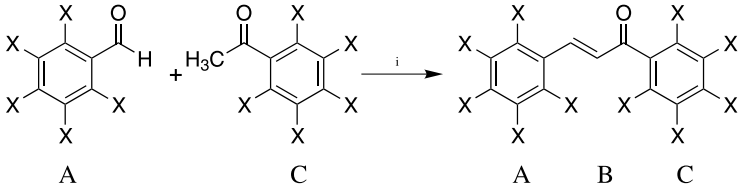

Scheme 1. Generalized synthetic scheme for the preparation of enone derivatives. Reagents and conditions: (i) 10–40% KOH, EtOH, 5–10 °C. Let stir ~4 h at room temperature. X = H, Cl, F, OCH_3, CF_3, OH, NH_2, CH_3, $CH(CH_3)_2$, NO_2, phenyl, OBn, and CH_2COOH; A and C ring systems = benzene, 1-napthalene, 2-napthalene, 2-pyridine, 3-pyridine, 5-benzo[1,3]dioxole, 2-furan, 2-pyrrole, and 9-anthracene.

3.2. 1-Phenyl-3-(3-pyridyl)propenone (23)

Benzoylmethylene triphenylphosphorane (1.95 g, 5.14 mmol) was added to a stirring solution of pyridine-3-carboxaldehyde (500 mg, 4.67 mmol) in 7.0 ml of dry methylene chloride. The solution was allowed to stir at room temperature overnight. It was then concentrated on a rotoevaporator, which afforded the crude product. Recrystallization from diethyl ether resulted in 295 mg (31.9%) of the expected product (light-yellow powder): mp 102.7–103.7 °C. ^{1}H NMR (250 MHz) δ 8.86 (s, 1H), 8.64–8.63 (d, 1H), 8.06–7.93 (m, 3H), 7.83–7.76 (d, 1H), 7.63–7.49 (m, 4H), 7.39–7.34 (m, 1H); ^{13}C NMR (62.7 MHz) 190.0, 151.3, 150.1, 141.1, 137.9, 134.8, 133.3, 130.6, 126.9, 126.7, 124.0 ppm.

3.3. 1,3-Di(2-pyridyl)propenone (24)

Concentrated hydrochloric acid (2.1 ml) was added dropwise to an ice-cold (5-10 °C) solution of pyridine-2-carboxaldehyde (442 mg, 4.13 mmol) and 2-acetylpyridine (500 mg, 4.13 mmol) in 10.3 ml ethanol. The reaction mixture was stirred for 1.5 h at 5–10 °C. The flask was then removed from the ice and allowed to stir at room temperature for an additional 6 h. At this time, the solution was placed back into the ice bath and neutralized using 40% sodium hydroxide. A standard ether extraction/workup yielded the crude product, which was chromatographed on a silica gel column using 2:1 hexane/ethyl acetate to afford 253 mg (29.1%) of a light-yellow solid that turned light green upon standing (purity was unaffected): mp 66.2–67.2 °C. ^{1}H NMR (250 MHz) δ 8.68–8.60 (m, 3H), 8.12–8.09 (d, 1H), 7.88–7.40 (m, 5H), 7.23–7.19 (m, 1H); ^{13}C NMR (62.7 MHz) 189.9, 154.0, 153.9, 148.1, 143.1, 137.1, 136.9, 127.2, 125.1, 124.8, 124.4, 122.2 ppm.

3.4. 2,2′,3,3′,4,4′,5,5′,6,6′-Decafluorochalcone (27)

Sodium hydroxide (100 mg) was added to 4.2 ml of water and 3.2 ml of 95% ethanol. This solution (1.9 ml) was placed in an ice bath and 2,3,4,5,6-pentafluoroacetophenone (500 mg, 2.38 mmol) along with 2,3,4,5,6-pentafluoroaldehyde (467 mg, 2.38 mmol) was added to the reaction flask. After stirring for approximately 2 h at room temperature, a yellow solid precipitated and was filtered. The solid was recrystallized from ethanol (two times) to afford 550 mg (59.5%) of a white powder: mp 58.4–59.0 °C. ^{1}H NMR (250 MHz) δ 7.66–7.59 (d, 1H), 7.37–7.30 (d, 1H); ^{13}C NMR (62.7 MHz) 183.1, 148.3, 146.9, 144.2, 142.6, 140.1, 136.1, 132.1, 130.3, 114.2, 109.7 ppm.

3.5. 1-(1-Naphthyl)-3-phenylpropenone (42)

An aqueous 40% potassium hydroxide solution (10 ml) was added drop wise to a chilled (5–10 °C), stirring flask containing a mixture of 1-napthylethanone (1.2 g, 10 mmol) and benzaldehyde (1.56 g, 10 mmol) in 15 ml of ethanol. A viscous oil formed after stirring for 3 hours and the reaction mixture was extracted with ether (3 portions, ~10 ml). After the organic layers were concentrated under reduced pressure, the oil remained and purified with silica gel using a 9:1 hexanes:ether solution to afford 850 mg (32.9%) of yellow flakes: mp 105.5–106.7 °C. ^{1}H NMR (250 MHz) δ 8.37–8.33 (m, 1H), 8.03–8.00 (d, 1H), 7.95–7.90 (m, 1H), 7.81–7.78 (d, 1H), 7.68–7.49 (m, 6H), 7.45–7.41 (m, 2H), 7.36–7.29 (d, 1H); ^{13}C NMR (62.7 MHz) 195.9, 146.1, 137.3, 134.8, 134.0, 132.5, 131.8, 130.9, 129.2, 128.9, 127.5, 126.7, 125.6, 124.7 ppm.

3.6. 1-(1-Naphthyl)-3-(2-naphthyl)propenone (44)

An aqueous 40% potassium hydroxide solution (10 ml) was added dropwise to an ice cold (5–10 °C), stirring flask containing a mixture of 1-naphthalen-1-yl-ethanone (1.70 g, 10 mmol) and naphthalene-2-carbaldehyde (1.56 g, 10 mmol) in 15 ml of ethanol. After stirring for approximately 3 h, a viscous oil formed. The oil was allowed to sit at room temperature for 2 days, at which time a solid formed. The crude product was recrystallized (two times) from ethyl acetate to afford 1.39 g (45.1%) of yellow flakes: mp 83.5–84.3 °C. ^{1}H NMR (250 MHz) δ 8.41–8.37 (m, 1H), 8.05–7.74 (m, 9H), 7.63–7.51 (m, 5H), 7.47–7.40 (d, 1H); ^{13}C NMR (62.7 MHz) 195.7, 146.2, 137.3, 134.8, 134.1, 133.5, 132.3, 131.8, 131.0, 130.7, 129.0, 128.8, 128.7, 128.0, 127.7, 127.4, 127.3, 127.0, 126.7, 125.6, 124.7, 123.8 ppm.

3.7. 1-Phenyl-3-(2-pyrrolyl)propenone (58)

To a solution of acetophenone (630 mg, 5.26 mmol) and pyrrole-2-carboxaldehyde (500 mg, 5.26 mmol) in 2.1 ml of ethanol was added 0.5 ml of an aqueous 10% sodium hydroxide solution at room temperature. After stirring overnight, the solution was filtered. The resulting precipitate was recrystallized from 90% ethanol to afford 500 mg (48.5%) of the pure product: mp 136.6–137.4 °C. ^{1}H NMR (250 MHz) δ 9.19 (b s, 1H), 8.01–7.97 (m, 2H), 7.81–7.75 (d, 1H), 7.60–7.45 (m, 3H), 7.22–7.16 (d, 1H), 7.01 (s, 1H), 6.73 (s, 1H), 6.36–6.33 (m, 1H); ^{13}C NMR (62.7 MHz) 190.9, 135.1, 132.6, 128.8, 128.5, 123.5, 116.0, 115.6, 111.7 ppm.

3.8. 2-(2,6-Dichlorobenzylidene)tetralone (62)

An aqueous 40% potassium hydroxide solution (10 ml) was added dropwise to an ice cold (5–10 °C), stirring flask containing a mixture of 1-tetralone (1.46 g, 10 mmol) and 2,6-dichloro-benzaldehyde (1.75 g, 10 mmol) in 30 ml of ethanol. The solution turned purple following the addition of the basic solution. After stirring for approximately 4 h, a viscous purple oil formed. Column chromatography with silica gel using 9:1 hexane/ethyl acetate as the eluent afforded a yellow oil. Upon standing at 4 °C, a solid formed and was recrystallized from ethanol yielding 2.00 g (66.0%) of faint-yellow platelets: mp 73.8–75.6 °C. ^{1}H NMR (250 MHz) δ 8.20–8.17 (d, 1H), 7.60 (s, 1H), 7.50 (t, 1H), 7.40–7.37 (m, 3H), 7.26–7.19 (m, 2H), 2.97 (t, 2H), 2.86 (t, 2H); ^{13}C NMR (62.7 MHz) 187.0, 144.1, 139.7, 134.8, 134.2, 133.7, 133.4, 130.8, 129.6, 128.5, 128.2, 127.2, 28.8, 28.0 ppm.

3.9. SVR cell studies

The endothelial cell proliferation assays used in this study were developed by Arbiser et al.[19] at Emory University. Primary murine endothelial cells, garnered from adult C57BL/6 mice, were infected with an ecotropic retrovirus encoding the simian virus 40 (SV40) large T 58-3 allele coupled with a resistance to neomycin. The resulting cells were selected in a solution of Dulbecco's modified Eagle's medium (DMEM), 5% fetal calf serum, and 0.6 mg/ml geneticin. The clone cells were stained with 1,1′-dioctadecyl-3,3,3′,3′-tetramethylindocyanine perchlorate coupled to acetylated low density lipoprotein (diI-Ac-LDL). Fluorescence microscopy was used to identify the positive clones. The clone MS1 was expanded and infected with an additional retrovirus, which encoded for activated H-ras (mutant allele at glycine-12 and threonine-59) as well as hygromycin resistance. The resulting, immortalized endothelial cell line was designated SVR.

For use in the in vitro assays, the SVR cells were plated 10,000 cells/well in a 24-well cell culture dish (polystyrene). The cells were cultured for approximately 24 h at 37 °C in 10% DMEM (0.5 ml/well) under a 5% CO_2 atmosphere. During the initial 24 h incubation period, the living cells adhered themselves to the bottom of their individual wells. The DMEM growth media were then aspirated and replaced with 0.5 ml of a fresh 10% DMEM solution containing 1, 3, or 6 μg/ml of the individual test compounds. Each drug was dissolved in a minimal amount of dimethylsulfoxide (DMSO) in order to prepare stock test solutions (10 mg/ml) from which the appropriate drug dilutions were obtained. For this reason, each plate utilized one column (three wells) as a DMSO control group for each specific drug concentration tested by the assay. A single microliter of each individual stock solution was added to 1 ml of fresh incubation medium resulting in a 10 μg/μl solution. 0.1, 0.3, and 0.6 ml of these solutions were then added to additional 0.9, 0.7, and 0.4 ml aliquots of 10% DMEM, respectively, in order to generate the appropriate concentrations for testing. After the addition of the drug solutions, the cell culture plates were allowed to incubate for an additional 48 h under the same conditions used during the initial incubation period. At the end of the 2 day period, each of the wells was aspirated and then washed with 0.5 ml of Dulbecco's Phosphate Buffered Saline (DPBS) and aspirated again in order to remove any dead cells or lingering DMEM. The remaining, live cells were removed from the bottom of each well using 0.5 ml of a 1X trypsin-EDTA solution (0.5% trypsin, 0.53 mM EDTA-4Na in HBSS without Ca, Mg, or $NaCO_3$). The enzymatic activity of the trypsin was neutralized by the addition of 0.5 ml of fresh 5% DMEM after approximately 8 min. After each well was thoroughly mixed to insure homogeny, 0.5 ml of the media from each well was mixed with 9.5 ml of Coulter's Isoton II balanced electrolyte solution and the total number of cells/well was counted using a Coulter Z1 cell counter. The total cell count of each test well was then compared to the DMSO control well for each concentration. The percent inhibition of cell growth was calculated from these values.

References and notes

1. Ammon, H. P.; Wahl, M. *Planta Med.* **1991**, *57*, 1.
2. Stoner, G. D.; Mukhtar, H. *J. Cell. Biochem. Suppl.* **1995**, *22*, 169.
3. Sharma, O. P. *Biochem. Pharmacol.* **1976**, *25*, 1811.
4. Toda, S.; Miyase, T.; Arichi, H.; Tanizawa, H.; Takiyano, Y. *Chem. Pharm.* **1985**, *33*, 1725.
5. Srimal, R. C.; Dhawan, B. N. *J. Pharm. Pharmacol.* **1973**, *25*, 447.
6. Satoskar, R. R.; Shah, S. J.; Shenoy, S. G. *Int. J. Clin. Pharmacol. Ther. Toxicol.* **1986**, *24*, 651.
7. Mazumder, A.; Raghavan, K.; Weinstein, J.; Kohn, K. W.; Pommer, Y. *Biochem. Pharmacol.* **1995**, *49*, 1165.
8. Eigner, D.; Scholz, D. *J. Ethnopharmacol.* **1999**, *67*, 1.
9. Huang, M. T.; Lou, Y. R.; Ma, W.; Newmark, H. L.; Reuhl, K. R.; Conney, A. R. *Cancer Res.* **1994**, *54*, 5841.
10. Rao, C. V.; Rivenson, A.; Simi, B.; Reddy, B. S. *Cancer Res.* **1995**, *55*, 259.
11. Conney, A. H.; Lysz, T.; Ferraro, T.; Abidi, T. F.; Manchand, P. S.; Laskin, J. D.; Huang, M. T. *Adv. Enzyme Regul.* **1991**, *31*, 385.
12. Huang, M. T.; Ma, W.; Lu, Y. P.; Chang, R. L.; Fisher, C.; Manchand, P. S.; Newmark, H. L.; Conney, A. H. *Carcinogenesis* **1995**, *16*, 2493.
13. Huang, M. T.; Deschner, E. E.; Newmark, H. L.; Wang, Z. Y.; Ferraro, T. A.; Conney, A. H. *Cancer Lett.* **1992**, *64*, 117.
14. Arbiser, J. L.; Klauber, N.; Rohan, R.; van Leeuwen, R.; Huang, M. T.; Fisher, C.; Flynn, E.; Byers, H. R. *Mol. Med.* **1998**, *4*, 376.
15. Robinson, T. P.; Ehlers, T.; Hubbard, R. B.; Bai, X. H.; Arbiser, J. L.; Goldsmith, D. J.; Bowen, J. P. *Bioorg. Med. Chem. Lett.* **2003**, *13*, 115.
16. Furness, M. S.; Robinson, T. P.; Ehlers, T.; Hubbard, R. B., IV; Arbiser, J. L.; Goldsmith, D. J.; Bowen, J. P. *Curr. Pharm. Des.* **2005**, *11*, 357.
17. Bowen, J. P.; Robinson, T. P.; Ehlers, T.; Goldsmith, D.; Arbiser, J. Chalcone and its analogs as agents for the inhibition of angiogenesis and related disease states. PCT Int. Appl. WO0146110, June 28, 2001.
18. Shim, J. S.; Kim, J. H.; Cho, H. Y.; Yum, Y. N.; Kim, S. H.; Park, H. J. *Chem. Biol.* **2003**, *10*, 695.
19. Arbiser, J. L.; Moses, M. A.; Fernandez, C. A.; Ghiso, N.; Cao, Y.; Klauber, N.; Frank, D.; Brownlee, M.; Flynn, E.; Parangi, S.; Byers, H. R.; Folkman, J. *Proc. Natl. Acad. Sci. U.S.A.* **1997**, *94*, 861.